Overcoming Optical Gaps: Evaluating SAR–Optical Consistency for Cotton Phenology

Alp Eren Furkan Demirci, Filiz Sunar

ITU, Faculty of Civil Engineering, Geomatics Engineering Department, 34467 Maslak Istanbul, Türkiye
(demirci15, fsunar)@itu.edu.tr

ABSTRACT:

Reliable monitoring of cotton phenology is challenged by cloud-induced gaps in optical satellite observations, especially during key growth stages. This study evaluates the temporal consistency between C-band Synthetic Aperture Radar (SAR) features from Sentinel-1 and vegetation indices from Sentinel-2 across eleven adjacent cotton fields in Didim, Türkiye, during the 2024 season. Sentinel-1 dual-polarization (VV, VH) backscatter, polarimetric decomposition parameters (Entropy, Alpha, Anisotropy), and Stokes-derived metrics (e.g., g_0) were extracted from Single Look Complex (SLC) data processed in SNAP. Sentinel-2 Level-2A imagery was used to compute seven vegetation indices (NDVI, EVI, ARVI, NDRE, NDWI, MSAVI, GCI) after cloud masking via the Scene Classification Layer. A ±2-day temporal matching strategy aligned SAR and optical acquisitions, enabling inter-field correlation analysis. Results show strong, consistent relationships between VH backscatter and chlorophyll–biomass–oriented indices, with NDVI–VH (mean r = 0.930), ARVI–VH (0.928), and EVI–VH (0.924) exhibiting synchronized seasonal trajectories. Stokes g_0 correlated highly with biomass- and moisture-sensitive indices, including MSAVI (0.863), EVI (0.860), and NDWI (0.858), highlighting its utility as a cloud-resilient surrogate for canopy status. In contrast, H/A/α parameters demonstrated weak coupling to optical indices (e.g., GCI–Entropy mean r = 0.115), reflecting their sensitivity to structural scattering mechanisms not directly linked to pigment dynamics. These findings indicate that combining VH backscatter and g_0 with optical indices provides a robust, cloud-tolerant monitoring framework, while H/A/α offer complementary structural diagnostics. The proposed approach is scalable using free, global datasets and is transferable to other phenology-driven agricultural monitoring applications.

Keywords: SAR-Optical Fusion, Vegetation Indices, Sentinel-1, Sentinel-2, Polarimetric Decomposition.

1. Introduction

Cotton is one of the most economically significant crops in the global textile and agriculture sectors, with Türkiye ranking among the top producers (TURKSTAT, 2023). Monitoring cotton growth across its complex phenological cycle—emergence, vegetative growth, flowering, boll development, and maturation—is critical for ensuring optimal yield, timely interventions, and sustainable management. Traditional field-based monitoring, while informative, is often constrained by spatial limitations, labour intensity, and susceptibility to weather conditions. In this context, satellite-based remote sensing has emerged as a reliable and scalable alternative for crop observation.

Among remote sensing platforms, optical satellites such as Sentinel-2 provide spectral information useful for estimating vegetation vigour and health through indices like Normalized Difference Vegetation Index (NDVI), Normalized Difference Red Edge (NDRE), and Enhanced Vegetation Index (EVI). However, optical sensors are sensitive to atmospheric disturbances, particularly cloud cover, limiting their usability during critical growth phases. Conversely, Sentinel-1 offers weather-independent C-band SAR imagery with dual polarization (VV and VH), enabling reliable observations even under overcast conditions. Furthermore, polarimetric SAR decomposition techniques—such as entropy, anisotropy, and alpha angle—along with Stokes parameters, provide structural and dielectric insights that are closely linked to crop development. Beyond basic backscatter, polarimetric SAR decomposition techniques provide deeper insight into crop structure and scattering mechanisms (Demirci, 2025). Metrics such as entropy (H), alpha angle (α), and anisotropy (A) describe the randomness, dominant scattering type, and balance of secondary mechanisms within the canopy, respectively—parameters that can reveal changes in plant geometry, layering, and water distribution not directly visible in optical data. Stokes parameters further quantify polarization purity and the balance between co- and cross-polarized returns, offering an integrated measure of canopy structure and dielectric properties. By combining these polarimetric features with conventional backscatter, SAR observations extend beyond simple intensity measurements, providing complementary structural and biophysical information critical for understanding crop phenology.

Recent advances in space technology support the integration of SAR and optical data for robust agricultural monitoring. However, most studies have focused on backscatter intensity or classification outputs, with limited attention to the temporal dynamics of polarimetric SAR metrics. Moreover, the application of such approaches in Türkiye remains underexplored, despite its prominence in global cotton production. This study addresses these gaps by integrating Sentinel-1 and Sentinel-2 data to evaluate the temporal consistency of SAR and optical vegetation indices over 11 cotton fields in the Aegean region of Türkiye. Sentinel-1 SAR data were used to extract dual-polarization backscatter values and polarimetric indicators such as entropy, alpha angle, anisotropy, and Stokes parameters. Concurrently, Sentinel-2 imagery was used to derive vegetation indices including NDVI, NDRE, and EVI. All observations were aligned with key phenological stages of cotton, enabling an in-depth temporal analysis of biophysical signal consistency and their interrelations.

2. Study Area

This research was conducted over 11 neighbouring cotton fields situated in Didim, a coastal district in Aydın Province, western Türkiye (Figure 1). The region, located along the Aegean Sea, experiences a typical Mediterranean climate defined by hot, dry summers and mild, wetted winters (TSMS, 2023). During the main cotton growing season, which spans roughly from May through September, daytime temperatures often exceed 34 °C. In contrast, winter months see average temperatures around 14 °C, with most annual rainfall occurring between November and March. These climatic conditions—prolonged warmth, high

solar exposure, and off-season rainfall—create a highly favourable environment for cultivating thermophilic crops such as cotton, especially when supplemented with irrigation.
The selected cotton fields form a compact, continuous block that was deliberately chosen to minimize spatial variability caused by differences in soil composition, microclimate, or farming practices. Their geographic coherence enhances the consistency of remote sensing analyses by providing a relatively uniform biophysical context. The study area lies between latitudes 37.54° and 37.58° N and longitudes 27.25° and 27.30° E, a few kilometres inland from the Aegean coast. The fields are located within the lower basin of the Büyük Menderes River, benefiting from both natural soil fertility and access to irrigation infrastructure. Surrounding land use includes other agricultural parcels and low-density rural infrastructure, contributing to a typical semi-rural landscape. Throughout the study period, the selected parcels were continuously cultivated with cotton, providing an ideal setting for tracking seasonal crop dynamics. All subsequent analyses are focused on these 11 parcels, leveraging high-resolution, multi-temporal data from Sentinel-1 and Sentinel-2 to observe phenological development and structural changes throughout the growing season.

Figure 1. Geographic distribution of the 11 cotton fields in Didim, Aydın Province, Türkiye. The red outlines indicate individual field boundaries used in this study.

3. Materials and Methods

3.1 Materials

This study utilized multi-source satellite observations to monitor cotton fields located in Didim, Aydın, during the 2024 growing season (May–October). The primary datasets included both SAR and optical imagery from the Sentinel constellation:
- Sentinel-1 Level-1 Single Look Complex (SLC) and Ground Range Detected (GRD) data were used for structural and moisture-related analysis. A total of 17 SLC scenes (Interferometric Wide swath, VV/VH dual polarization) were downloaded from the Copernicus Open Access Hub (https://dataspace.copernicus.eu). Additional GRD-format images were retrieved via Google Earth Engine (GEE), limited to ascending orbits to ensure acquisition consistency. Sentinel-1 GRD pre-processing included thermal noise removal, radiometric calibration, and terrain correction using Shuttle Radar Topography Mission (SRTM-30) data. The final sigma nought (σ°) values were converted to decibel (dB) scale.
- Sentinel-2 Level-2A Surface Reflectance (SR) data were also acquired from GEE, covering 13 spectral bands (B1–B12, including B8A). These bands span the visible, near-infrared, red-edge, and shortwave infrared regions. High-resolution bands (10 m) such as B2 (Blue), B3 (Green), B4 (Red), and B8 (NIR) were used for vegetation index calculation, including NDVI, NDRE, and EVI. Red-edge bands (B5, B6, B7, B8A) were also utilized for enhanced vegetation analysis.
All imagery was acquired within the 2024 cotton phenological cycle and systematically aligned with field-specific growth stages. Data processing and extraction workflows were implemented using SNAP, Google Earth Engine Python API, and QGIS.

3.2 Methods

The methodological framework comprises standardized pre-processing, vegetation index derivation shown in Table 1, temporal synchronization, and statistical correlation analyses conducted at the inter-field level. Sentinel-1 and Sentinel-2 datasets were collected for the 2024 cotton growing season (May 20 – November 10). Sentinel-1 data were processed in ESA SNAP, while Sentinel-2 Level-2A products were handled using a Python-based pipeline with cloud masking via the Scene Classification Layer (SCL). The full process flow is illustrated in Figure 2.

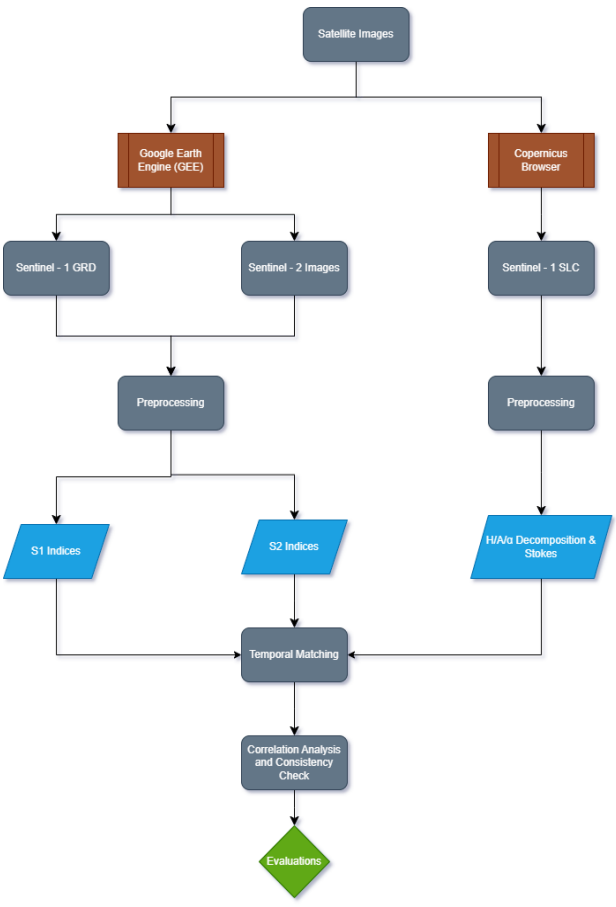

Figure 2. Methodological framework used.

Two polarimetric product categories were derived:
1. The Cloude–Pottier H/Alpha/Anisotropy decomposition: This eigenvalue-based analysis was applied to the C2 coherency matrix to extract Entropy (H), Mean Alpha Angle ($\bar{\alpha}$), and Anisotropy (A), which respectively characterize scattering randomness, dominant scattering mechanisms, and secondary scattering contributions (Cloude, 2007).

2. Stokes Parameters and derived metrics: Using SNAP's CP Stokes operator, a suite of 14 variables was computed, including g_0–g_3 components; degree of polarization (DoP); degree of

circularity (sin 2χ); ellipticity (χ); circular and linear polarization ratios; linear relative phase (φ); polarization orientation angle (α_s); conformity coefficient (μ); and phase_phi (ϕ). These metrics collectively characterize polarization purity, scattering symmetry, and canopy structural complexity. (Braun & Veci, 2020)

These two outputs were terrain-corrected and exported for temporal analysis. The entire processing workflow implemented in SNAP is shown in Figure 3.

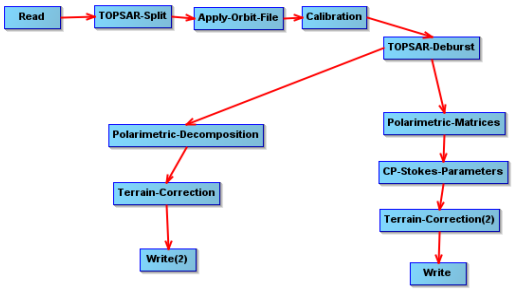

Figure 3. Sentinel-1 SLC data processing graph in SNAP, outlining the steps for polarimetric decomposition and Stokes parameter extraction.

In addition to standard backscatter coefficients (σVV, σVH) and polarimetric decomposition parameters, ratio- and difference-based SAR-derived vegetation indices were computed from dual-polarized Sentinel-1 data (Table 1) to enhance sensitivity to cotton canopy structure and scattering mechanisms. Here, σVV and σVH represent backscatter coefficients in linear power (not dB), converted from decibel values prior to ratio calculations (linear = 10^(dB/10)).

Index	Formula	Interpretation
SAR_ratio	σVH / σVV	Indicator of canopy density and volume scattering; higher values reflect stronger depolarized returns typical of dense vegetation.
SSD	σVH − σVV	Polarization-based structural contrast; large positive values suggest strong cross-polarized scattering from well-developed canopies.
SND	(σVH − σVV) / (σVH + σVV)	Normalized difference to reduce scale dependency; enables comparison across fields with different absolute backscatter levels.
SSR	(σVH / σVV) − (σVV / σVH)	Symmetric scattering ratio difference; emphasizes imbalances between co- and cross-polarized returns.
SSRM_VH	$(\sigma VH)^2$ / √(σVV)	Modified scattering ratio enhancing VH sensitivity under dense canopy conditions.
SSRM_VV	$(\sigma VV)^2$ / √(σVH)	Modified scattering ratio emphasizing VV response under sparser canopy conditions.

Table1. SAR-based vegetation indices computed from dual-polarized Sentinel-1.

Sentinel-2 Level-2A surface reflectance products were processed to derive vegetation indices, using bands B2 (Blue), B3 (Green), B4 (Red), B5 (Red Edge), B8 (NIR), and B11 (SWIR) (Table 2).

Index	Formula	Interpretation
Normalized Difference Vegetation Index (NDVI)	$\frac{B8-B4}{B8+B4}$	It measures vegetation greenness and photosynthetic activity.
Enhanced Vegetation Index (EVI)	$\frac{2.5*(B8-B4)}{B8+6*B4-7.5*B2+1}$	It estimates vegetation vigor while minimizing soil and atmospheric effects.
Normalized Difference Red Edge (NDRE)	$\frac{B8-B5}{B8+B5}$	It measures chlorophyll content, especially during later growth stages.
Normalized Difference Water Index (NDWI)	$\frac{B8-B11}{B8+B11}$	It indicates canopy water content and plant moisture status.
Modified Soil-Adjusted Vegetation Index (MSAVI)	$\frac{2*B8+1-\sqrt{(2*B8+1)^2-8*(B8-B4}}{2}$	It reduces soil background effects and enhances vegetation detection in sparse canopies.
Green Chlorophyll Index (GCI)	$\frac{B8}{B3}-1$	It estimates leaf chlorophyll concentration, linked to nitrogen status.
Atmospherically-Resistant Vegetation Index (ARVI)	$\frac{B8-(2*B4-B2)}{B8+(2*B4-B2)}$	It measures vegetation greenness under variable aerosol conditions.

Table 2. Optical vegetation indices derived from Sentinel-2 data (Kaufman & Tanré 1992; Gao 1996).

Pearson correlation coefficients were computed between Sentinel-1–derived features (SAR backscatter indices, Cloude–Pottier decomposition parameters, and Stokes-based metrics) and Sentinel-2 vegetation indices. Analyses were field-specific to preserve spatial integrity.

A second-level consistency check was applied across the 11 fields to assess the generalizability of observed correlations. Metrics such as mean, standard deviation, min–max range, and interquartile range (IQR) were calculated for each index pair. Only relationships with high mean correlation and low variability were considered spatially consistent and reliable for cotton monitoring.

4. Results

Normalized seasonal trajectories revealed distinct, phenologically consistent patterns for both optical and SAR-derived metrics across the 11 cotton fields. The main characteristic trends observed were as follows:

- Optical metrics: NDVI and EVI rose rapidly during vegetative growth (late May–early July), peaked during flowering and early boll development (mid-July–late August), and gradually declined toward senescence in October. NDWI fluctuated markedly during flowering, driven by irrigation cycles and soil moisture variations.

During early growth, MSAVI remained stable, effectively reducing soil background effects before full canopy closure.

- SAR metrics: In early emergence, SAR backscatter was dominated by soil returns, limiting vegetation sensitivity to vegetation. From mid-season onwards, backscatter increased notably as canopy structure and biomass density developed. VH-polarized backscatter and volume-scattering–sensitive ratios (e.g., VH/VV) showed the highest responses during peak canopy closure, while VV-polarized backscatter exhibited more gradual seasonal dynamics.

To provide a qualitative overview prior to the time-series plots, four cloud-free dates aligned with key phenological phases of the 2024 season (20 May–10 November) were selected: early vegetative (late May–early June), rapid vegetative/early flowering (early–mid July), flowering/boll development (mid–late August), and senescence/defoliation (mid-October). For each date, Sentinel-2 RGB and NDVI images, as well as Sentinel-1 VH and Stokes g_0 images, are presented in Figure 4.

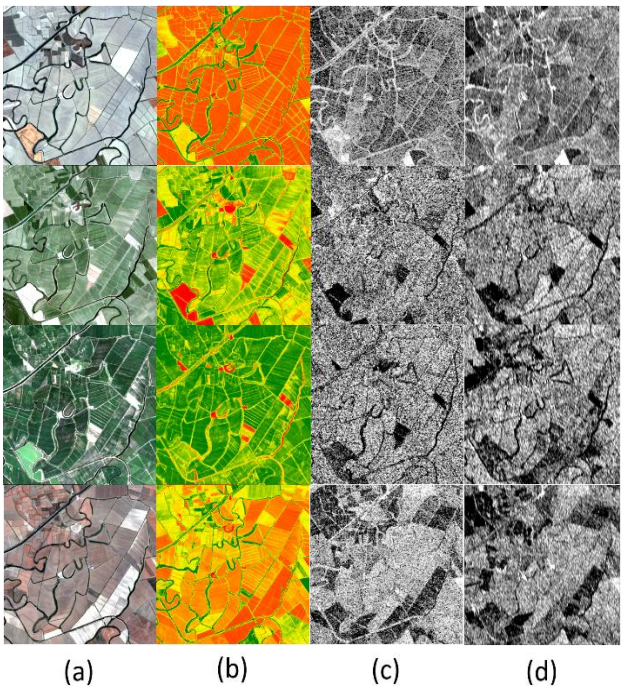

Figure 4. Seasonal images over the study fields: (a) Sentinel-2 RGB, (b) NDVI, (c) Sentinel-1 VH (dB), (d) Stokes g_0 (linear). Rows correspond to four phenological dates.

4.1 Statistical Analysis and Time Series Patterns

4.1.1 Optical and SAR metrics

Correlation analysis between optical and SAR metrics revealed strong and phenologically consistent relationships. The strongest correlations were observed between NDVI, EVI, ARVI and VH (vh_mean_linear) backscatter, with mean seasonal r-values above 0.92 across all fields (Table 3). In contrast, the lowest correlations were found for SAR ratio metrics, all below 0.35.

Sentinel 2 – Sentinel 1 (GRD)	
Pair	**Mean(r)**
NDVI | VH_mean_linear	0.930
ARVI | VH_mean_linear	0.928
EVI | VH_mean_linear	0.924
EVI | SAR_ratio	0.339
NDRE | SAR_ratio	0.330
NDWI | SAR_ratio	0.312

Table 3. Top three and bottom three mean correlations (r) between Sentinel-2 vegetation indices and Sentinel-1 backscatter/ratio metrics, calculated across 11 cotton fields.

These metrics followed the same growth-linked pattern — starting low in early growth, rising sharply during vegetative expansion, peaking at maximum biomass in late July–early August, and declining toward harvest. The high correlations with VH backscatter can be explained by its sensitivity to volume scattering from randomly oriented canopy elements such as leaves, stems, and bolls. At peak growth, cotton's dense canopy enhances VH depolarization, while optical indices respond to simultaneous increases in chlorophyll, leaf area index, and photosynthetically active biomass. This shared sensitivity to structural and physiological changes explains the close temporal alignment and strong statistical relationship.

Figure 5 illustrates these dynamics using normalized time series of NDVI, EVI, ARVI (Sentinel-2) together with VH_mean_linear (Sentinel-1) across all 11 fields, highlighting their synchronized seasonal patterns.

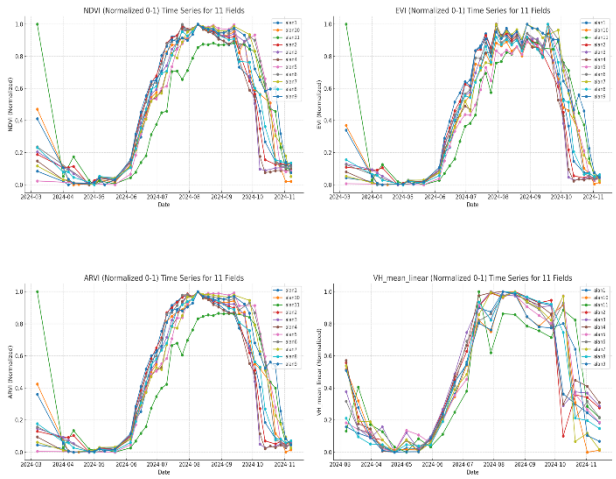

Figure 5. Normalized seasonal patterns of NDVI, EVI, and ARVI derived from Sentinel-2 imagery, and VH (vh_mean_linear) backscatter from Sentinel-1, across eleven cotton fields during the 2024 growing season.

4.1.2 Optical and Stokes Parameters

Across n = 240 matched pairs, g_0 exhibited strong mean correlations with MSAVI, EVI, and NDWI (Table 4). Their seasonal trajectories were synchronized, with a rapid increase during canopy expansion, a plateau near peak biomass, and a decline during senescence (Figure 6). As g_0 represents the total backscattered power in a dual-pol system, integrating co- and cross-polarized returns, it is sensitive to both canopy structural thickening and water-related dielectric variations.

Sentinel 2 – Stokes Parameters	
Pair	**Mean(r)**
NDWI | g_0	0.933
EVI | g_0	0.924
MSAVI | g_0	0.899
MSAVI | circular_polarization_ratio	0.006
NDWI | linear_relative_phase	-0.004
NDVI | linear_relative_phase	0.003

Table 4. Top three and bottom three mean correlations (r) between Sentinel-2 vegetation indices and Sentinel-1 Stokes parameters/derived ratios across 11 cotton fields.

Figure 6 illustrates this correspondence, showing normalized time series of MSAVI, EVI, NDWI (Sentinel-2) together with g_0 (Sentinel-1 Stokes parameter) across all fields. The curves demonstrate synchronized growth-peak-decline patterns, highlighting the role of g_0 as an integrated structural-moisture indicator for cotton monitoring.

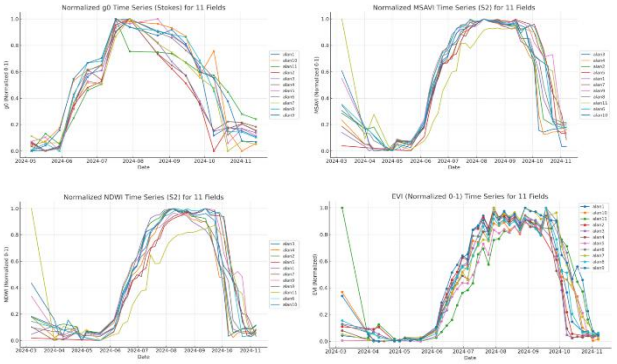

Figure 6. Temporal dynamics of SAR-derived g_0 (Stokes parameter) and Sentinel-2 vegetation indices (MSAVI, NDWI, and EVI) for 11 cotton fields in Didim, Aydın during the 2024 growing season.

This strong correspondence exists because g_0 represents the total radar backscatter power from the canopy, combining contributions from both co- and cross-polarized returns. In cotton, the microwave scattering signal is mainly controlled by two factors: the dielectric properties of vegetation (closely linked to water content) and the geometric complexity of the canopy (determined by leaf area index, leaf orientation, stem density, and boll formation).

During early growth, scattering is dominated by soil returns since the sparse canopy interacts only weakly with the radar signal. As plants develop, increasing leaf biomass and vertical layering lead to a denser distribution of scatterers. Randomly oriented leaves and fine branches enhance cross-polarized volume scattering, while stems and larger structural components strengthen co-polarized returns. g_0, being the sum of both, reflects this combined structural and dielectric effect more fully than a single polarization.

EVI and MSAVI are sensitive to biomass accumulation and canopy chlorophyll, which increase in parallel with the radar-observed structural complexity. NDWI tracks changes in leaf and stem water content, directly affecting vegetation dielectric properties and thus backscatter intensity. As biomass and water content increase during vegetative and reproductive phases, both optical indices and radar scattering follow similar seasonal trajectories.

At peak canopy closure, scattering reaches its maximum, producing strong depolarization and increased g_0 values, while optical indices also reach their seasonal maxima. This parallel continues until senescence, when declining leaf water content and leaf drop reduce both canopy structure and backscatter, leading to decreases in the optical indices as well. This joint sensitivity to water status, biomass, and canopy structure explains the close temporal and statistical agreement observed across all fields.

4.1.3 Optical and Decomposition Parameters

The polarimetric decomposition parameters—Entropy (H), Anisotropy (A), and Alpha (α)—show consistently weak correlations with optical vegetation indices (Table 5). These parameters are designed to describe the scattering mechanisms at microwave scales: α indicates scattering type (low ≈ surface, mid ≈ volume, high ≈ double-bounce), H increases with randomness or mixing of mechanisms, and A highlights the secondary scattering contribution when H is intermediate. The weak coupling suggests that while decomposition captures physical scattering diversity, it does not directly translate to the optical signals dominated by pigment, water, and biomass dynamics.

Sentinel 2 – H/a/α Decomposition	
Pair	**Mean(r)**
GCI | Entropy_mean	0.115
GCI | Alpha_mean	0.112
MSAVI | Alpha_mean	0.084
NDWI | Entropy_mean	0.015
NDVI | Entropy_mean	0.012
EVI | Alpha_mean	0.02

Table 5. Top three and bottom three mean correlations (r) between Sentinel-2 vegetation indices and polarimetric decomposition parameters (Entropy, Alpha, Anisotropy) across 11 cotton fields.

Figure 7 presents normalized time series of the optical GCI and SAR decomposition metrics α, H, and A across all fields. As described above, these parameters capture scattering type, randomness, and secondary contributions, respectively. Since they respond primarily to radar-scale structure and moisture redistribution (e.g., row and stem geometry, boll development, canopy re-organization) rather than pigments, their seasonal dynamics diverge from visible–NIR indices. Across the 11 fields and matched dates, correlations remain weak (Table 5), confirming that decomposition parameters encode scattering processes largely orthogonal to chlorophyll- or water-driven optical signals.

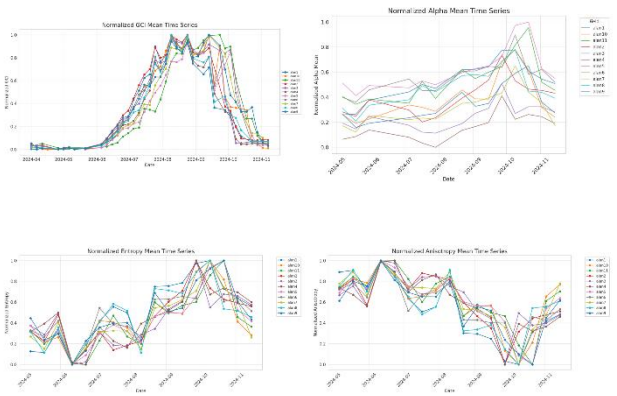

Figure 7. Temporal evolution of Sentinel-2 GCI and SAR decomposition parameters (α, H, A) for 11 cotton fields in 2024, normalized to 0–1.

5. Conclusion

This study evaluated relationships between Sentinel-2 vegetation indices and Sentinel-1 backscatter, Stokes, and decomposition parameters across eleven cotton fields in 2024. Three main findings were identified:

- Cross-polarized VH backscatter provides a reliable proxy for phenological dynamics, closely aligned with chlorophyll- and biomass-sensitive indices (NDVI, ARVI, EVI).
- Stokes g_0, representing total backscattered power, serves as a robust indicator of canopy status under cloudy conditions, correlating with MSAVI, EVI, and NDWI by jointly reflecting structural and water-related changes.
- Decomposition parameters (H, A, α) show weak correlations with optical indices, highlighting their role as complementary descriptors of canopy scattering geometry rather than pigments.

Operationally, VH in combination with NDVI/EVI/ARVI is suited for phenology-aware monitoring; g_0 is valuable as an alternative during optical gaps; and H/A/α may be reserved for diagnosing structural reorganizations not captured by greenness indices.

The workflow is scalable using free, global data and standard platforms (SNAP, GEE). However, conclusions are limited to one season, one region, C-band dual-pol data, ±2-day pairing, and sparse ground observations. Future work will plan to expand to multiple seasons and regions with in-situ validation (LAI, biomass, water status, yield), test multi-frequency and quad-pol acquisitions, refine temporal alignment and incidence-angle normalization, integrate thermal and red-edge features, and develop fusion approaches that combine VH and g_0 with optical indices, while incorporating H/A/α as structural information.

References

Braun, A., & Veci, L. (2020). *Sentinel-1 Toolbox: Polarimetry with RADARSAT-2 — Tutorial (Rev. Jan 2020)*. ESA/STEP.

Cloude, S. R. (2007): *The Dual Polarisation Entropy/Alpha Decomposition: A PALSAR Case Study*. In Science and Applications of SAR Polarimetry and Polarimetric Interferometry (3rd International Workshop, Frascati, Italy, 22–26 January 2007).

Copernicus Data Space Ecosystem. (n.d.): *Copernicus Sentinel Data Access*. European Space Agency. Retrieved from https://dataspace.copernicus.eu

Demirci, A. E. F. (2025): *Evaluating the temporal consistency of SAR and optical vegetation indices for cotton monitoring using Sentinel-1 and Sentinel-2* [Master's thesis, Istanbul Technical University].

Gao, B.C. (1996). NDWI—A normalized difference water index for remote sensing of vegetation liquid water from space. Remote Sensing of Environment, 58(3), 257–266. https://doi.org/10.1016/S0034-4257(96)00067-3

Gorelick, N., Hancher, M., Dixon, M., Ilyushchenko, S., Thau, D., & Moore, R. (2017): Google Earth Engine: Planetary-scale geospatial analysis for everyone. *Remote Sensing of Environment*, 202, 18–27. https://doi.org/10.1016/j.rse.2017.06.031

Kaufman, Y. J., & Tanré, D. (1992): Atmospherically resistant vegetation index (ARVI) for EOS-MODIS. IEEE Transactions on Geoscience and Remote Sensing, 30(2), 261–270. https://doi.org/10.1109/36.134076

Turkish State Meteorological Service (TSMS) (2023): *Climate data for Aydın Province*. Retrieved from https://www.mgm.gov.tr

Turkish Statistical Institute (TURKSTAT). (2023): Crop production statistics. Retrieved from https://data.tuik.gov.tr